Review and Recent Developments in DC Arc Fault Detection

Xiu Yao
Department of Electrical Engineering
University at Buffalo
Buffalo, NY 14260
xiuyao@buffalo.edu

Jin Wang
Department of Electrical and Computer Engineering
The Ohio State University
Columbus, OH 43210
Wang.1248@osu.edu

Daniel L. Schweickart
Air Force Research Laboratory
Aerospace Systems Directorate
Wright Patterson AF Base, OH 45433
daniel.schweickart@us.af.mil

***Abstract*—This paper presents a brief review of recent dc arc fault modeling and detection methods. The goal is to examine state-of-the-art technologies and to identify future research and development needs of dc arc fault protection in modern dc networks. For dc arc modeling, the focus is given to external characteristic equations which model the arc with electrical parameters. Moreover, models of the random high frequency components in arc current and their applications will be reviewed and discussed. Then, selected dc arc fault detection techniques are reviewed and compared. Preliminary results from a robustness study for a wavelet based detection algorithm under noisy environments are presented. The status of a draft SAE standard being developed on 270 Vdc arc fault detection and validation tests for aircraft is briefly discussed.**

Keywords—dc arc, arc model, fault detection, noise

I. Introduction

With the development and implementation of dc based power systems, dc arc fault protection becomes an inevitable challenge for the safe operation in various applications including electric vehicles (EV), more electric aircraft (MEA), photovoltaic(PV) plants, data center, dc microgrids, and other systems that require high voltage dc buses. DC arc fault detection is considered more challenging than its ac counterpart, due to the absence of zero crossings, and the low fault current of high impedance, series dc arc faults which can increase the complexity in fault detection. While some of the ac protection techniques can be used in dc systems with certain modifications, dc arc fault detection is particularly challenging. For automobile industry, dc arc faults were a concern when moving from 14 Vdc to 42 Vdc system voltage to accommodate higher power requirements [1]. The dc bus voltage in EV is around several hundred volts, presenting more arc fault hazards. Similarly, the 270 Vdc system in MEA, to reduce size and weight, is faced with similar dc arc fault challenges. Among all the applications, dc arc fault detection in PV systems is the most mature, with products and standards already established [2-4]. On the contrary, the standards for MEA or EV applications are currently in development.

The goal of this paper is to review the recent development on dc arc fault detection (not limited by specific applications), to examine the state-of-the-art technologies and to identify future research and development needs of dc arc fault protection in modern dc networks. One salient trend of dc system development is that the system complexity has been increasing, leading to more diverse sources, with varying operating points and modes. As a result, the fault detection, especially for high impedance, series dc arcing faults, becomes more and more challenging. Current and future dc systems are calling for reliable, flexible and "smart" dc arc fault detection techniques.

In this paper, arc modeling and arc detection in the published literature and patents are briefly reviewed. The importance of arc modeling has been emphasized with the increased complexity of the dc systems, in order to achieve accurate fault studies and power flow analyses. The second half of this paper focuses on the authors' recent effort on evaluating the robustness of wavelet decomposition based detection techniques against various noise types and levels commonly found in power systems. The status of a draft SAE standard being developed on 270 Vdc arc fault detection and validation tests for aircraft is then discussed.

II. DC Arc Model

Arc models have been under research since the last century. However, earlier models are focused on voltage - current (V-I) equations and Finite Element Analysis (FEA), which describes the arc not as a fault, but as a normal process that could occur during the opening of a mechanical circuit breaker or arc furnace operation [5-6].

A FEA model is obtained by simulating the detailed physical processes in the plasma discharge. Although very beneficial to the study of the physical properties of an arc, the

This work was sponsored by AFRL/RQQE via University of Dayton Research Institute contract FA8650-12-D-2224(TO0002).

FEA model has not been utilized for the study of arc fault effects in a circuit. The V-I equation can be useful to examine the steady state characteristics of an arc, generally relating arc current and arc voltage with one equation, with several coefficients determined by electrode materials, shapes, gap lengths, etc. It can be used to predict the steady state fault response of a dc system. However, V-I equations neglect an important feature of arc: it is a plasma discharge channel associated with varying high frequency components that are dependent upon molecular collision-dominated random processes.

For detection purposes, high frequency components can play an important role. On one hand, they provide the opportunity to detect the existence of an arc fault by monitoring the high frequency components in either current or voltage measurements. The propagation of high frequency components in a system can allow for sensors in a remote location and may reduce the number of local sensors needed. On the other hand, high frequency component propagation may also cause cross talking and unwanted tripping in a neighboring non-faulted section of the circuit. This complexity makes the modeling of high frequency components very important to facilitate the study of their impact in various systems under different conditions.

In general, three types of models are involved: the steady state model (V-I), the high frequency component model, and the transient model. Each of these models simulates an aspect that is essential to the analysis of arc fault response. Each type of model can be used by itself or concurrently with another, depending on the specific application.

A. Steady steady model (V-I equations)

The dc arc fault is often categorized as a high impedance fault, because the arc channel exhibits a substantial amount of resistance that cannot be neglected. Therefore, V-I equations are adopted to describe the nonlinear resistive characteristics of the arcing. V-I equations are generally achieved empirically through curve fitting of the arc voltage and current under a large number of testing points.

Depending on the experimental condition, several V-I equations have been proposed with somewhat similar forms. A comprehensive review of the earlier equations proposed can be found in [6]. A summary of some of these equations along with a recent modified equation is presented in Table I, where L represents the gap length which is used to approximate the arc length. A, B, C, and D are coefficients to be determined by experimental conditions [7].

Most of these equations are proposed for high power applications with a large current and gap length range. The Modified Paukert equation incorporated gap length in smaller steps than the original Paukert equation with smaller current and gap length ranges. It is proposed to model dc arc faults in the scale that can be found in modern dc power systems with dc bus voltages of several hundred volts.

Another feature incorporated in the Modified Paukert equation is that the gap length L has a nonlinear impact to V_{arc}, as represented by the term $I_{arc}^{\ b+dL}$ in the denominator. Details of this derivation can be found in [8].

TABLE I. V-I EQUATIONS IN PREVIOUS STUDIES

Name	Equation	Experimental condition
Ayrton	$V_{arc} = A + BL + \frac{C + DL}{I_{arc}}$	Carbon electrodes
Steinmetz	$V_{arc} = A + \frac{C(L + D)}{I_{arc}^{\ 0.5}}$	Carbon and magnetite electrodes
Nottingham	$V_{arc} = A + \frac{B}{I_{arc}^{\ n}}$	n is related to electrode material; L: 0.039 to0.39 in
Paukert	$V_{arc} = \frac{a}{I_{arc}^{\ b}}$	L: 0.039 to 7.78 in Iarc: 0.3 to 100 kA
Modified Paukert	$V_{arc} = \frac{a + cL}{I_{arc}^{\ b+dL}}$	L: 0.04 to 0.12 in Iarc: 3 to 25 A

B. High frequency component model

The randomness of arc current, represented by the noise-generating high frequency components, is caused by the plasma discharge in the dc arcing channel. The molecule and coulomb collision in the plasma channel is essentially a random process, which leads to a Gaussian probability distribution of the ac component of the arc current. [9] uses a zero-mean Gaussian noise function to describe the voltage fluctuation of arc. From [9], [7] further studied the Gaussian distribution of an arc current under different conditions. The ac component of the arc current is fitted into a Gaussian distribution expressed by the following equation:

$$f_x = \frac{1}{\sigma\sqrt{2\pi}} e - \frac{(x-\mu)^2}{2\sigma^2} \quad (1)$$

This study shows the feasibility of using a Gaussian distribution to describe the arc current randomness and further showed that the distribution is quantitatively associated with the dc component level of arc current. The Gaussian distribution fitting of measurement noise can also be separated from the arcing current randomness.

A different approach is adopted in [10] where a randomly generated value is added to the arc resistance equation:

$$R_{gap} \approx \frac{V_{dc}}{I_{load}} e^{2\alpha(q-1)}\Omega \quad (2)$$

and a random function is used to generate jitter, q, as follows:

$$q^{k+1} = q^k + rand()^{10} \quad (3)$$

In [11], colored wideband noise is proposed to model the small-signal behavior of arcing. While a Gaussian function describes the probability distribution with respect to the value, the "color" indicates the signal power distribution over a wide frequency range. It is generally assumed that the random noise of a dc arc is a pink noise or brownian noise [12]. Pink noise can often be generated by filtering Gaussian white noise. As can be seen, the high frequency component of arcing can be modeled from both the probability of amplitude and the frequency domain distribution aspects.

C. *Transient model*

The definition of an arc transient depends on how the arc is generated. For UL 1699B recommended test setup, two electrodes are placed with a predetermined gap length, with fine steel wool placed in a polycarbonate tube. When the circuit is energized, a current will flow through the steel wool which shorts the two separated electrodes. The current will then melt the steel wool, similar to the way a fuse would work. The melting of steel wool will provide ionization of the air and then initiate arcing. In this case, the arc transient is very short, which is indicated by the sudden current drop in the load circuit and the voltage increase across the electrodes, as can be seen from Fig. 1(a). The measured arc voltage is composed of two parts: the anode and cathode voltage, and the column voltage. The anode and cathode voltage is related to the electromotive force (EMF), occurs at the layer very close to electrodes [13]. It is essential to the initiation and sustaining of the arcing channel. The anode and cathode voltage is generally independent of the gap length and external circuit, but is dependent on the electrode material. The column voltage on the other hand is caused by the current flowing through the resistive arcing channel and is dependent on both the current and gap length. Therefore, for an arc generated by the steel wool with fixed gap length, the arc voltage becomes stable very quickly, as shown in Fig. 1 (a). The model of this short transient has not been well studied. However, the di/dt produced during this transient has been widely used as a fault indicator in detecting series dc arc faults.

Another common approach to generate an arc is by pulling apart two electrodes which were originally making contact, until reaching a predetermined gap length or until the arc is naturally extinguished while the circuit is energized. In this case, the voltage across arc is still composed by the anode and cathode voltage, and column voltage. Although the cathode and anode voltage is established very quickly and remains constant during the entire pulling process, the column voltage keeps increasing during the puling process due to the increase of gap length. In this case, the transient process has two parts, the initial sudden current and voltage step change, and the quasi-stationary stage where arcing is established but still growing, as can be seen in Fig. 1(b). A transient model for this drawn arc is presented in [10], where exponential functions are used to describe the arc voltage, current, and resistance development during the entire elongation of the arc. The arc resistance model is shown in (2).

III. Review of DC Arc Fault Detection

DC arc fault detection techniques have three facets. The first part is based on sensors and the measurement quantities which they produce. The most commonly used measurements include current and voltage quantities from current transducers, Hall Effect sensors, etc. With the raw measurement data, fault signatures are calculated as the second step of the detection process. The term "signatures" are commonly referred to as "indictors" or "features" in the literature as well. These terms are generally interchangeable. The requirements of an effective fault signature are twofold. On one hand, the difference between a fault condition signature and a normal condition signature should be as great as possible; on the other hand, the difference among normal operating condition signatures should be as minimal as possible. These requirements are to make sure that the fault signature will indicate fault occurrence without confusing it with normal operations with a similar system response. The last step is the detection algorithm with signature parameters as input, where one or more signatures are analyzed to make the final decision of a definite or "positive" arc fault detection. Signatures and algorithms can be realized with analog circuits and/or microprocessor controllers.

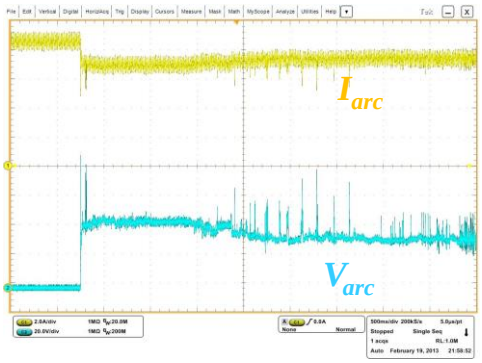

(a) Arc voltage and current with steel wool setup

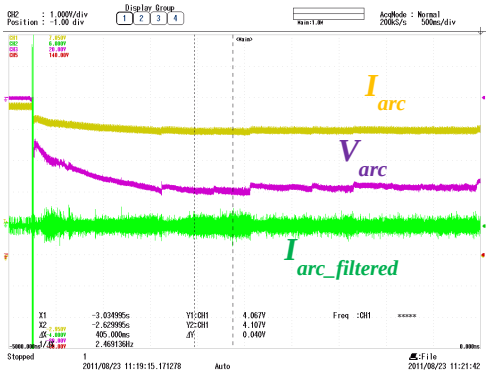

(b) Arc voltage and current with the pulling procedure

Fig. 1. Examples of arc voltage and current waveforms

In this remaining section, recent dc arc fault detection techniques from literatures and patents are reviewed. Review of relatively earlier techniques can be found in [7, 14]. Instead of categorizing these techniques based on the domain of fault signatures, they will be divided into three categories corresponding to the three aspects discussed above. The rationale behind this arrangement is that with the increasing complexity of modern dc systems, the importance of sensor deployment and more sophisticated detection algorithms is also increasing and therefore should be discussed separately.

A. *Measurement and sensors*

As mentioned earlier, the most commonly measured signals are the current and voltage in certain points of the circuit. Current is also more commonly used than voltage. Part of the reason might be that unless the potential fault location is known, more voltage sensors are required than current sensors to cover the entire circuit. The measurements used in recent patents and literatures are listed as follows:

- Current transformer with band pass filter [15, 16]
- Current sensors in multiple locations [17]
- Current sensor based on Hall Effect comprising with ring or toroid of magnetic material [18]
- Both current and voltage sensors [19-22]
- Input dc current and voltage, output ac current and voltage measurement of a PV inverter [20]
- AC and dc component of the inverter input voltage and current [21]
- DC and ac component of source and bus voltage and current [22]
- Load voltage only [23, 24]
- Air core transformer [25]
- Two or more Rogowski coils with frequency response of 15 MHz [26]
- Electromagnetic (EM) signals collected using loops or antennas [27]

To summarize, voltage measurement in most cases is to be used in conjunction with current measurement except in [23, 24]. In this case, load voltage is measured assuming that the arc fault occurring upstream may cause a voltage drop at the load. While the technology of the voltage sensor is usually not discussed, different types of current sensors have been specified in some of the studies. Current sensors for ac component include current transformers and Rogowski coils, with bandpass filters in some cases, while Hall Effect is generally used to measure the dc component when needed. The measurement of dc component can be useful to decide the operating point of the circuit [21]. In [27], loops or antennas are used to collect the radiofrequency characteristics of the arc fault.

B. Fault signatures/indicators

Some of the fault signatures proposed in recent literatures and patents are listed below:

- Average pulse count, average pulse duration fluctuation, average pulse duration, and average pulse count fluctuation [15]
- Absolute value of the 1 kHz to 100 kHz content of current measurement [16]
- The number of current signal peaks [17]
- Original current, voltage, or power [16, 18-20]
- Dynamic behavior of voltage and current, relationship between voltage and current, averaged value [20]
- Derivative or rate of change of current [20,25]
- Absolute sum of the FFT of arc current below 10 kHz [21]
- RMS value of two level wavelet decomposition [22]
- Four level wavelet decomposition of load voltage waveform [23, 24]
- Correlation of current measured by Rogowski coil [26]
- 1.5 – 30 MHz frequency band of measured EM signals [27]

It can be seen that the time domain analysis of arc current or voltage measurements is still widely used, in the form of di/dt, average, counting of peaks, peak durations, etc. The key of using FFT as a frequency domain feature is that the frequency range has to be carefully selected to include the effect of the arc fault, but exclude that from normal operations such as switching frequency. Wavelet decomposition, as a time-frequency domain analysis tool, is suitable for fault detection. It has been applied to both current and voltage measurements. The selection of the mother wavelet is based on its similarity to the transient to be detected, while the number of decomposition levels is determined by the desired frequency band and limited by the computational capability. If the sampling frequency of the original measurement is higher, then more levels would be needed to achieve smaller range of frequency bands, which results in higher computation load. The computation load of frequency and time-frequency domain features are much higher than that of time domain analysis. It was shown in [8] that through certain arrangement of the computation algorithm, the computation load of wavelet decomposition can be lower than that of FFT.

C. Fault detection algorithms

Detection algorithms vary with the fault signatures. Some commonly used rationales are summarized below:

- Compare signatures with a threshold value or use comparators [15-17, 20, 22, 23-25]
- Compare signatures or measurements from multiple locations [18, 19]
- Fuzzy logic [21]
- Cross correlation [26]
- Support Vector Machine (SVM) [27]

Threshold values are critical to a majority of the detection techniques. The comparison of fault signature values to a threshold alone can be used to indicate fault. However, it is very difficult to choose a threshold value that works for all possible operating conditions. Therefore, more advanced and sophisticated algorithms such as SVM and fuzzy logic can be used as in [21, 27].

Based on the above review, dc arc detection in PV systems is relatively more developed than other dc systems, as evidenced by the majority of patents and products. Also, the first standards on dc arc fault detection were developed for PV applications including NEC and UL 1699 B. The NEC article 690.11 states that buildings with dc systems higher than 80 V are required to have arc fault interruption, while the UL standard outlines the test procedures and fault interruption requirement. Up until now, multiple products have passed these tests and become UL certified or listed. These products can be standalone interrupters or are integrated into PV inverters. Although this is a big step towards a reliable and robust protection to facilitate the development and adoption of dc systems in certain applications, the reality is that there are still gaps and challenges remaining to be solved. It should be noted that PV systems tend to have less switching-induced harmonic content due to normal operations than the dc systems in vehicles. According to an anonymous comparison study of different arc fault interrupters conducted in Sandia National Labs, even UL certified products can fail to detect an actual arc fault or experience unwanted tripping [28]. Some common

reasons for unwanted tripping are power or current step change, conducted dc/dc converter noise, ac noise prorogation, etc [28]. It is clear that there are still research gaps to achieve more reliable, robust, and fast dc arc fault interrupters for PV, and especially the dc systems in modern aerospace vehicles.

IV. Noise Sensitivity of Wavelet Based Detection

To investigate the impact of environmental noise to detection algorithms, this section studied the effectiveness of a wavelet transformation based detection algorithm proposed by the authors in [8] under noises that are commonly found in electrical systems, including wideband noise and repetitive sawtooth impulse noise. The wavelet based detection algorithm uses load current as the measured parameter. The load current can be measured using a Rogowski coil or using a Hall Effect sensor followed by a bandpass filter. In this study, a resistive current sensor followed by a 1.5-45 kHz bandpass filter was used. The sampling frequency is 200 kHz. The fault signature is the RMS value of frequency band (25-50 kHz) from wavelet decomposition for every 25 ms time. The calculated RMS value above 1.2~1.3 times the normal value is considered to be indicating an arc event.

A. *Wideband noise*

Wideband noise has energy component extended over a wide range of frequencies, such as white noise, pink noise, brown noise, etc. They are commonly introduced by electronic devices used in circuits or in measurement units. The impact of wideband noise has been studied in communication systems. The signal-to-noise ratio (SNR) is used to define noise level:

$$SNR = 10\log_{10}(\frac{S}{N})dB \tag{4}$$

where S is the amplitude of the original signal, which is the ac component of arc current $I_{arc,}$ N is the amplitude of noise I_{noise} where Gaussian white noise is used in this study as an example. In communication systems, SNR<20 dB is generally considered a bad scenario while SNR>60 dB is considered good. In electrical systems, more noise can be expected. Therefore, three SNR values were tested: 20, 10, and 3 dB, which correspond to I_{noise}/I_{arc} amplitude ratio of 0.01, 0.1, and 0.5, respectively.

The four waveforms in Fig. 3 are calculated RMS waveforms of the 25-50 kHz frequency band from a two level Daubechies decomposition. The obvious boost in the first RMS waveform after the arc occurs at around 0.6 seconds verifies the effectiveness of the arc fault detection. The second waveform in Fig. 3 shows the wavelet RMS results for the arc current with added 10 dB white noise, where the obvious difference can still be observed, showing that the chosen fault signature is effective even with 10 dB noise. The bottom two waveforms are to test whether the 10 dB white noise will cause unwanted tripping, where it can be seen that adding 10 dB white noise to the current pre-arcing does not result in an obvious change in the wavelet RMS waveform. However, when the SNR is reduced to 3 dB, the wavelet RMS will not be effective any more, as shown in Fig. 4. The detection of arc fault may still be possible with the spikes following the arcing initiation; however, the 3 dB noise is possible to cause unwanted tripping as shown in the bottom waveform in Fig. 4.

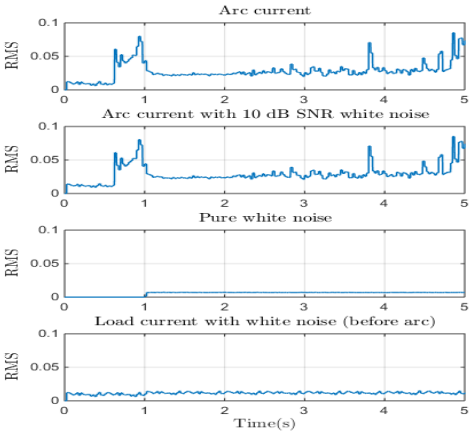

Fig. 3 Wavelet RMS waveforms with 10 dB noise

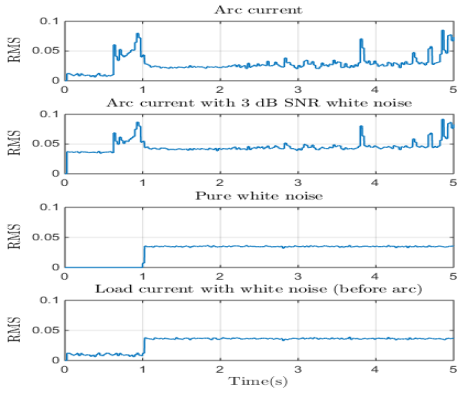

Fig. 4 Wavelet RMS waveforms with 3 dB noise

B. *Repetitive saw tooth impulse noise*

Repetitive electrical impulse noise can be caused by certain loads or household appliances [29]. They have mostly been investigated for their impact to communication systems. In this study, four groups of arc data are examined with different source voltage V_{source} and load current level I_{load}: 1) 120 V, 6 A; 2) 120 V, 25 A; 3) 175 V, 6 A; 4) 175 V, 25 A. Sawtooth impulse noise was used with 0.1 duty ratio. The noise frequencies examined include 100 Hz, 500 Hz, 1 kHz, 2 kHz, 5 kHz, 10 kHz, 20 kHz. Different noise amplitudes were tested until the noise amplitude became high enough that the detection algorithm was not effective any more. The following procedures were followed: 1) add noise to each of the four arc data waveforms; 2) find the maximum value of fault signature before arc fault occurs, Max_noarc; 3) find the minimum value of fault signature after arc fault occurs, Min_arc; 4) the percentage of the difference between the two is defined as:

$$P = \frac{Min\_arc - Max\_noarc}{Max\_noarc} \tag{5}$$

The noise limit is found when P reaches 30%. The noise limits for each case are plotted in Fig. 6, where the Noise Limit axis shows the noise amplitude when P reaches 30%.

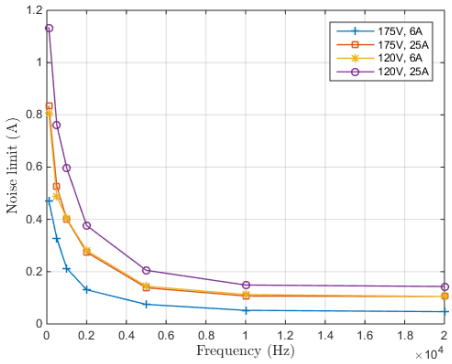

Fig.6 Noise limit plot for repetitive sawtooth waveform.

V. Conclusions

Recent developments of dc arc fault detection in the literature and patents have been reviewed. With the increase of dc system scale and complexity, more sophisticated detection algorithms have been proposed. It is concluded that better detection algorithms are still yet to be developed to cope with the more complicated environments containing spurious noise due to normal operating conditions. As it could be difficult to develop a single detection strategy to work well under all conditions, it is important to understand the limit and constraints in different applications. Therefore, a robustness study of wavelet decomposition based detection was carried out to investigate the broadband noise and repetitive impulse noise limits for one arc fault detection technique.

For PV applications, UL1699B (2011) already calls out the procedures and methods for dc arc-fault circuit protection verification. For aircraft applications, SAE-International is currently developing the test methods and procedures for validating the performance of arc-fault detection equipment for application in 270 Vdc systems. This standard, AS-6087, will specify the techniques for initiating the arcing, as well as the pass/fail criteria. To support the development of this standard, both the FAA and AFRL have been conducting arcing tests and generating arc signature records to aid the SAE's Arc Fault Detection working group, under the Aerospace Electrical Power and Equipment Committee, Power Management sub-committee, AE-7B.

References

[1] M. Naidu, T. J. Schoepf, and S. Gopalakrishnan, "Arc fault detection scheme for 42-V automotive DC networks using current shunt," IEEE Trans. Power Electron., vol. 21, no.3, pp. 633-639, May 2006.

[2] Outline of investigation for photovoltaic dc arc-fault circuit protection, UL1699B, 2011.

[3] National Electrical Code, 2011 Edition, NFPA70, National Fire Protection Association, Batterymarch, MA.

[4] SMA Solar Technology [online]. Available: http://www.sma-america.com.

[5] Q. G. Reynolds, and R. T. Jones, "Mathematical and computational modeling of the dynamic behavior of direct current plasma arcs," in 12th International Forroalloys Congress, Helsinki, Finland, 2010.

[6] R. Ammerman, T. Gammon, P. Sen, and J. Nelson, "DC-arc models and incident-energy calculations," IEEE Trans. Ind. Appl., vol. 46, no. 5, pp. 1810-1819, 2010.

[7] X. Yao, "DC Arc Fault Detection and Protection in DC Based Electrical Power Systems," Ph.D. Dissertation, The Ohio State University, 2015.

[8] X. Yao, L. Herrera, S. Ji, K. Zou, and J. Wang, "Characteristic study and time-domain discrete-wavelet-transform based hybrid detection of series DC arc faults," IEEE Trans. Power Electron., vol. 29, no. 6, pp. 3103-3115, June 2014.

[9] V. Terzija, et al., "EMTP simulation and spectral domain features of a long arc in free air," in Proceedings of 18th International Conference and Exhibition on Electricity Distribution, pp. 1-4, Turin, Italy, June 6-9, 2005.

[10] F. Uriarte, A. Gattozzi, J. Herbst, H. Estes, T. Hotz, A. Kwasinski, and R. Hebner, "A dc arc model for series faults in low voltage microgrids," IEEE Trans. Smart Grid, vol. 18, no. 5, pp. 2063-2070, Dec. 2012.

[11] C. Strobl, "Arc fault detection in DC microgrids," in Proceedings of 2015 IEEE First International Conference on DC Microgrids (ICDCM), pp. 181-186, Atlanta, GA, June 7-10, 2015.

[12] S. McCalmont, "Low cost arc fault detection and protection for PV systems," Tigo Energy, Inc., Los Gatos, CA, Contract 303 (2013): 275-3000.

[13] S. Ozcelik, and K. Moore, "Modeling, sensing and control of gas metal arc welding," Kidlington, Oxford: Elsevier Science, 2003.

[14] M. K. Alam, F. Khan, J. Johnson, and J. Flicker, "A Comprehensive Review of Catastrophic Faults in PV Arrays: Types, Detection, and Mitigation Techniques," IEEE Journal of Photovoltaics, vol. 5, no. 3, pp. 982-997, May 2015 .

[15] J. Kang, et al., "Noise propagation immunity of a multi-string arc fault detection device," U.S. Patent No. 20140195177 A1, July 10, 2014.

[16] L. Wang, et al., "DC arc fault detection circuit and protective device," CN Patent No. CN 203747363. July 30, 2014.

[17] J. K. Hastings, et al., "Direct current arc fault circuit interrupter, direct current arc fault detector, noise blanking circuit for a direct current arc fault circuit interrupter, and method of detecting arc faults," U.S. Patent No. 20110141644 A1, June 16, 2011.

[18] P. W. Dent, "Potential arc fault detection and suppression," U.S. Patent No. 9,190,836, Nov. 17, 2015.

[19] H. Behrends, et al., "Method and system for detecting an arc fault in a photovoltaic power system," U.S. Patent No. 9,046,588, June 2, 2015.

[20] M. Dargatz, and M. Fornage, "Method and apparatus for detection and control of dc arc faults," U.S. Patent No. 8,179,147, May 15, 2012.

[21] B. Grichting, et al., "Cascaded fuzzy logic based arc fault detection in photovoltaic applications," in proceedings of 2015 IEEE International Conference on Clean Electrical Power (ICCEP), pp. 178-183, June 16-18, 2015.

[22] X. Yao, et al., "Impact evaluation of series dc arc faults in dc microgrids," in Proceedings of 2015 IEEE Applied Power Electronics Conference and Exposition(APEC), pp. 2953-2958, Charlotte, NC, Mar. 15-19, 2015.

[23] R. S. Balog, "Method and System For Detecting Arc Faults and Flashes Using Wavelets," U.S. Patent No. 20140067291 A1, Mar. 6, 2014.

[24] Z. Wang, and R. S. Balog, "Arc Fault and Flash Signal Analysis in DC Distribution Systems Using Wavelet Transformation," IEEE Trans. Smart Grid, vol. 6, no. 4, pp. 1955-1963, July 2015.

[25] P. J. Handy, et al., "Apparatus and method for fault arc detection," DE Patent No. 10201304286 A1, Nov. 7, 2013.

[26] M. Rabla, et al., "Arc fault analysis and localisation by cross-correlation in 270 V dc," in Proceedings of 2013 IEEE 59th Holm Conference on Electrical Contacts (Holm 2013), Newport, RI, Sept. 22-25, 2013.

[27] K. Yang, et al., "A novel arc fault detector for early detection of electrical fires," Sensors, vol. 16, no. 4, pp. 1-24, 2016.

[28] J. Johnson, et al., "Arc-fault unwanted tripping survey with UL 1699B-listed products," in Proceedings of 2015 IEEE 42nd Photovoltaic Specialist Conference (PVSC), pp. 1-6, New Orleans, LA, June 14-19, 2015.

[29] J. Krejci, and T. Zeman, "Analyses and modeling impulse noise generated by household appliances," Advances in Electrical and Electronic Engineering, vol. 12, no. 1, pp. 20-29, Mar. 2014.